OPEN ACCESS
Scholars International Journal of Biochemistry
Abbreviated Key Title: Sch Int J Biochem
ISSN 2616-8650 (Print) |ISSN 2617-3476 (Online)
Scholars Middle East Publishers, Dubai, United Arab Emirates
Journal homepage: https://saudijournals.com

Original Research Article

Prevention of Cell Proliferation Signaling Via RNA Interference of *c-myc* Gene Expression in Colon Cancer *In-vitro*

Yousry Atef[1], Nasser H. Abbas[1], Adel A. Guirgis[1], Hany Khalil[2*]

[1]Department of Molecular Biology, Genetic Engineering and Biotechnology Research Institute, University of Sadat City, Sadat City, Egypt
[2]Professor, Department of Molecular Biology, Genetic Engineering and Biotechnology Research Institute, University of Sadat City, 79 Sadat City, Egypt

DOI: 10.36348/sijb.2023.v06i02.002 | **Received:** 02.01.2023 | **Accepted:** 09.02.2023 | **Published:** 19.02.2023

***Corresponding author:** Dr. Hany Khalil
Professor, Department of Molecular Biology, Genetic Engineering and Biotechnology Research Institute, University of Sadat City, 79 Sadat City, Egypt

Abstract

Colon cancer is a cancer begins in the large intestine (colon). Its aggression is due to late diagnosis, so poor prognosis and higher mortality rates are reported. Colon cancer has become a thorny research area that requires more examination of cellular pathways involved in its emergency. Based on this, we sought to check the biological role of cMyc in colon cancer cell proliferation through targeting its expression by a respective siRNA using CaCo-2 cell lines. Notably, the cytotoxic potential of cMyc knockdown was monitored by cell imaging using an inverted microscope, the production of lactate dehydrogenase (LDH) and viability of the transfected cells using MTT assay. The relative gene expression of c-myc and other related factors such as Raf-1 was investigated using quantitative real-time PCR (qRT-PCR). ELISA assay has been used to achieve the production of pro and anti-inflammatory cytokines released from transfected cells. Interestingly, the transfection with a new designed siRNA antagonist cMyc markedly decreased CaCo-2 cell viability rate in a dose-dependent manner compared with the transfection with specific siRNA antagonist Luciferase gene, which served as control. Likewise, number of survived cells significantly reduced following transfection with siRNA against c-myc, while the relative production of LDH significantly increased. Importantly, the cytotoxic effect of the transfection protocol showed neglected influence in normal colon epithelial cells (NCM-460 cell lines) indicating the selective regulation of colon cancer cell proliferation by transfection with siRNA targeting c-myc. Noteworthy, the knockdown efficiency of c-myc showed more than 80% inhibition of its expression in CaCo-2 cells transfected with the siRNA antagonist c-myc indicated by qRT-PCR. The relative gene expression of Raf-1 significantly decreased in c-myc knockdown cells, while the relative expression of both P53 and Caspase 3, as cell death indicators, significantly upregulated compared with control-transfected cells. Furthermore, the transfection with siRNA targeting c-myc markedly increased the production of interleukin 1 alpha (IL-1α) and IL-1β, as pro-inflammatory cytokines, while decreased the production of IL- 4 and IL-10, as anti-inflammatory cytokines. These data provide evidence for the involvement of c-myc gene expression in colon cancer cell proliferation and immune response during cancer development.

Keywords: Colon cancer, cMyc, Raf-1, Cell proliferation, Cells death, Immune response.

INTRODUCTION

The colon is the large intestine, by which the body draws out water and salt from solid wastes. Colon cancer is the third most common cause of cancer-related death in the U.S. Recently; colon cancer becomes an attractive field for researchers and scientists to check and find sufficient solutions for this endemic disease (Maher *et al*., 2020; Mohamed *et al*., 2022). Several cellular signaling have been identified in colon cancer, such as protein kinase C (PKC) and autophagosome formation (Islam *et al*., 2018; Devenport and Shah, 2019). PKC is a multifunctional family of serine/threonine kinase that modulates various cellular events such as cell growth, differentiation, and cell death. The activation of the PKC signaling pathway leads to, in some cases, autophagosome formation to protect the cells from apoptosis and regulates several cellular processes (Black and Black, 2013). Autophagosome formation is characterized by the

accumulation of double-membraned cytoplasmic vacuoles regulating degradation events and recycling of cellular contents by delivering cytoplasmic materials required for degradation to lysosomes (Abd El Maksoud *et al*., 2020).

Notably, the myc proto-oncogene has been recognized in the pathogenesis of most types of cancer. Activation of Myc in normal cells is believed to cause tumorigenesis through many genetically and epigenetically controlled mechanisms, including apoptosis, proliferative arrest, and senescence. When activated in a permissive genetic and epigenetic context, Myc controls these mechanisms, enforcing many cancer hallmarks such as DNA replication and transcription, protein synthesis, cellular proliferation, and relentless tumor growth altered cellular metabolism (Levens, 2010). Typically, Myc protein controls cancer cell providence by inducing stemness and avoiding cell senescence and apoptosis. Additionally, Myc arranges changes in the cancer microenvironment such as activation of angiogenesis and inhibition of the host immune response (Bellovin *et al*., 2013). Several cellular signaling regulate c-myc mRNA expression and promote cMyc protein stability, including phosphatidylinositol 3-kinase (PI3K)/AKT and mitogen-activated protein kinase (MAPK), RAS/RAF/MEK/ERK pathway. Evidence reported that the inhibition of the RAF/MEK/ERK pathway radically reduced cMyc expression and thus regulated cancer cell growth. However, several small agents have been identified as cMyc inhibitors, but none of them have yet been clinically tested (Zhao *et al*., 2015). On the other hand, knockout or even knockdown of the *Myc* gene leads to the recovery of fundamental checkpoint mechanisms, resulting in sustained cancer regression. Such regression propertied of depleted Myc is associated with cancer cells' proliferative arrest, differentiation, senescence, and apoptosis, as well as adjusting the tumor microenvironment, recruitment of an immune response, and preventing the angiogenesis (Madden *et al*., 2021).

Although scientists have started underlying colon cancer cells' development, much information and studies are required. Notably, colon cancer has different causes, and various signaling cascades are involved in cancer development. Recently, new tools and various techniques have been established to facilitate the analysis of cellular signaling and gene expression indicated in colon cancer cells. In this study, we aim to identify novel and efficacious compounds that can regulate colon cancer development with the minimum cytotoxic effects based on their influence on the cellular immune response in the colon cancer cell lines, such as CaCo-2 cells.

MATERIALS AND METHODS

Cell lines

Colon cancer epithelial cells CaCo-2 cell line was kindly provided by (VACSERA, Giza, Egypt) and were grown in Roswell Park Memorial Institute (RPMI) 1640 media supplemented with 25 mM HEPES, 4 mM L-glutamine, and 10% of heat-treated bovine serum albumin (BSA). The normal human colon mucosal epithelial cell line (NCM-460 cells) was grown in RPMI media that contains 4 mM L-glutamine and 10% BSA. All cell lines were incubated at 37°C and a relative humidity of 95% (Khalil *et al*., 2017b; Abd El Maksoud *et al*., 2019). The cultured cells' imaging was determined using inverted microscopy with a Zeiss A-Plan 10X.

Transfection Protocol

CaCo-2 cells were grown in a complete RPMI medium and were overnight cultured in 6-well plates with a confluency of about 80%. CaCo-2 cells were then transfected with different concentrations (100, 200, 300, 400, or 500ng/ml) of specific siRNA 5`-CAGCAGCUCGAAUUUCUUCCAGAUAUCU-3` that antagonist c-myc coding sequence using 20µl Lipofectamine LTX (Invitrogen, USA), prepared in 500 µl optimum media. Cells transfected with the same concentration of specific siRNA 5`-AACUUACGCUGAGUACUUCGA-3` that antagonist luciferase gene sequence was severed as control-transfected cells. According to the manufacturer's protocol, the transfection reagent with siRNA was incubated for 30 minutes at room temperature with a regular vortex. Then CaCo-2 cells were transfected with 500 µl of transfection mixture and incubated for 6 hrs. Finally, the media was removed from transfected cells, fresh media was added, and plates were incubated for two days. The knockdown efficiency of cMyc and the relative expression of indicated genes were monitored in transfected cells using qRT-PCR (Abd El Maksoud *et al*., 2020).

Proliferation Assay

To monitor the viability of transfected cells, cells were seeded in triplicate in 96-well plates at $10x10^3$ cells per well or in duplicate in a 6-well plate at $10X10^4$ cells per well. Cell morphology was assessed using an inverted microscope. The number of living cells was accounted by using a hemocytometer. Accordingly, the old media was removed, and then the cells were washed twice by PBS and trypsinized by adding an appropriate volume of trypsin followed by 3 min incubation at 37°C. Finally, an appropriate volume of complete RPMI media was added to the trypsinized cells, and the number of cells was accounted using the inverted microscope (Taher *et al*., 2021).

Cytotoxic concentration 50% (CC_{50})

The transfection of specific siRNA targeting cMyc gene expression was tested for their anticancer properties and calculated the potential CC50 in CaCo-2

cells. Accordingly, the cells were cultured in triplicate in 96-well plates in a density of $10X10^3$cells/well and were incubated overnight at 37°C and humidity conditions. The cells were transfected with the indicated concentrations of specific siRNA followed by overnight incubation. The cell viability rate and cytotoxic concentration were monitored by using MTT colorimetric assay kit (Sigma-Aldrich, Germany). Thus, the old media was removed from Transfected cells seeded in 96-well, and PBS was used to wash the cells, and then 100 µl complete RPMI media was added to each well. Subsequently, 10 µl MTT solution was added to each well, and the plate was incubated for 2 hours at 37°C. Finally, 100 µl SDS-HCl solution was added to each well in the plate which then was incubated for 4 hrs at 37°C. Cell viability was then assessed based on the amount of converted water-soluble MTT to an insoluble formazan which is then solubilized and determined by optical density at 570 nm (El-Fadl *et al*., 2021).

Lactate dehydrogenase (LDH) production

LDH assay kit (Abc-65393) was used to assess LDH production in the fluid media collected from cultured-transfected cells. According to the manufacturing procedures, 100µl of lysed cells was incubated with 100 µl LDH reaction mix for 30 min at room temperature. A plate reader was used to quantify LDH production at OD 450 nm. The relative LDH production is calculated by dividing the mean values of treated cells on the values of nontreated cells and indicated by fold change (Khalil, 2012; Khalil *et al*., 2019).

Enzyme-linked immunosorbent assay (ELISA)

According to the manufacture protocol, cells cultured in 96-well plates were overnight incubated. Then the cells were treated with different concentrations of each siRNA followed by an incubation period of (0, 6, 12, 24, 36, 48, and 72 hrs). At each time point, the cells were lysed using 1X cell lysis buffer (Invitrogen, USA). Then, 100 µl of the lysed cells were transferred into the ELISA plate reader and incubated for 2 hrs R.T. with 100 µl control solution and 50µl 1X biotinylated antibody. Then 100 µl of 1X streptavidin-HRP solution was added to each well of samples and incubated for 30 min in the dark. 100 µl of the chromogen TMB substrate solution was added to each well of samples and incubated for 15 min at R.T., away from the light. Finally, 100 µl stop solution was added to each well of samples to stop the reaction. The absorbance of each well was measured at 450 nm (Khalil *et al*., 2017a; Elimam *et al*., 2020; Maher *et al*., 2020).

Quantitative real-time PCR (qRT-PCR)

The quantification analysis of gene expression was detected using qRT-PCR. The total cellular RNA was obtained using TriZol (Invitrogen, USA) and purified using an RNA purification kit (Invitrogen, USA). Complementary DNA (cDNA) was synthesized from 1 µg of total RNA using reverse transcriptase (M-MLV, Promega, USA). The relative expression of c-myc, Raf-1, P53, and Caspase 3 (Casp3) mRNA were achieved using QuantiTect-SYBR-Green PCR Kit (Qiagen, USA) and the specific primers listed in Table 1. The housekeeping glyceraldehyde 3-phosphate dehydrogenase (GAPDH) expression level was used for normalization in the real-time PCR data analysis. The PCR reaction system contained 10 µl SYBR green, 0.25 µl RNase inhibitor (25 U/µl), 0.2 µM of each primer, 2 µL of synthesized cDNA, and nuclease-free water up to a final volume of 25 µL. The following PCR conditions were used; 94°C for 5 min, 35 cycles (94°C for 30 sec, 60°C for 15 sec, 72°C for 30 sec) (Khalil *et al*., 2019; El-Fadl *et al*., 2021; Hamouda *et al*., 2021).

Data analysis and prediction tools

The Freiburg RNA online tool, IntaRNA program, was used to predict the possible interactions between designed siRNA and cMyc gene sequence. Notably, since IntaRNA uses a heuristic to enable the low runtime, the provided energies are (close) upper bounds. Only interaction energies below or equal to 0 are visualized, and missing data (subsequences without predicted interactions) are also depicted with an energy of 0. The cMyc sequence was obtained from National Library of Medicine (https://www.ncbi.nlm.nih.gov). Delta-Delta Ct equations were used to quantify mRNA form delivered data of qRT-PCR assay based on the following equations: (1) delta-Ct = Ct value for gene-Ct value for GAPDH, (2) (delta–delta Ct) = delta Ct value for experimental –delta Ct for control), (3) Quantification fold change = (2-delta-delta ct) (Rao *et al*., 2013; Khalil H *et al*., 2017; Elimam *et al*., 2020). The student's two-tailed t-test was exploited for the statistical analysis. P-value ≤ 0.05 was considered statistically significant.

Table 1: Oligonucleotides sequences used for quantifying mRNA of indicated genes

Description	Primer sequences 5'-3'
cMyc-sense	TGAGGAGACACCGCCCAC
cMyc- antisense	CAACATCGATTTCTTCCTCATC TTC
Raf-1-sense	TTTCCTGGATCATGTTCCCCT
Raf-1 antisense	ACTTTGGTGCTACAGTGCTCA
P53-sense	GCGAGCACTGCCCAACAACA
P53-antisense	GGTCACCGTCTTGTTGTCCT
Casp3-sense	GGACAGCAGTTACAAAATGGA TTA
Casp3- antisense	CGGCAGGCCTGAATGATGAAG
GAPDH-sense	TGGCATTGTGGAAGGGCTCA
GAPDH-antisense	TGGATGCAGGGATGATGTTCT

RESULTS

Short interference RNA (siRNA) designing and interfering with cMyc

The IntaRNA program was used as a fast and accurate prediction tool for interactions between two RNA molecules. The IntaRNA has been designed to predict mRNA target sites for given non-coding RNAs (ncRNAs) like eukaryotic microRNAs (miRNAs) or bacterial small RNAs (sRNAs), but can also be used to predict other types of RNA-RNA interactions. A respective siRNA (28 nucleotides in length) targeting the c-myc coding sequence has been designed based on an appropriate sequence containing 50% CG nucleotides and without repetition of one nucleotide four times. As shown in Figure 1A, the combined plots reveal the intermolecular indexed pair between the indicated siRNA sequence (Query) and c-myc (Target). Interestingly, two main binding sites have been provided within 714-740 and 881-890 in the coding sequence of c-myc. The diagram presented in Figure 1B provides insights into the overall siRNA-c-myc interaction abundance. To this end, a minimal energy profile is provided for both sequences of each query-target pair is considered in Figure 1C. It visualizes for a given pairing of sequences for each sequence position the minimal energy of any siRNA-c-myc interaction that can form between these two RNAs. Notably, the minimal power for each intermolecular index pair is provided in a heat map style to track whether or not they can create alternative interactions exclusively (overlapping regions) or in conjunction.

Figure 1: Schematic representation of designed siRNA with c-myc coding sequence (A) The binding site and potential interaction of the designed siRNA (Query) and c-myc coding sequence (Target). (B) The exact position of pairing sequences into the c-myc coding sequence. (C) The table presents the required energy of each binding site between siRNA and cMyc coding sequence

Antagonism c-myc gene expression depletes cell viability of CaCo-2 cells

To illustrate the cytotoxic potential of siRNA transfection and to select the appropriate concentration of siRNA, cell viability rate and relative lactate dehydrogenase (LDH) production were achieved upon transfection using MTT assay and LDH production kit, respectively. As shown in Figure 1A and Table 2, the

mean absorbance values of CaCo-2 cell viability rate were notably reduced in a dose-dependent manner of transfected siRNAs, showing a sufficient concentration of 100ng/ml of siRNA that antagonist c-myc. In contrast, the most toxic concentration was 500ng of siRNA targeting c-myc, while transfection with siRNA antagonist Luciferase showed neglected influence in cell viability rate. Furthermore, the relative LDH production was significantly increased in CaCo-2 cells upon transfection of 100ng/ml siRNA antagonist c-myc compared with the same concentration of siRNA targeting Luciferase (Figure 2B and Table 3). Together, these data confirm the anticancer properties of targeting c-myc with the newly designed siRNA in colon cancer.

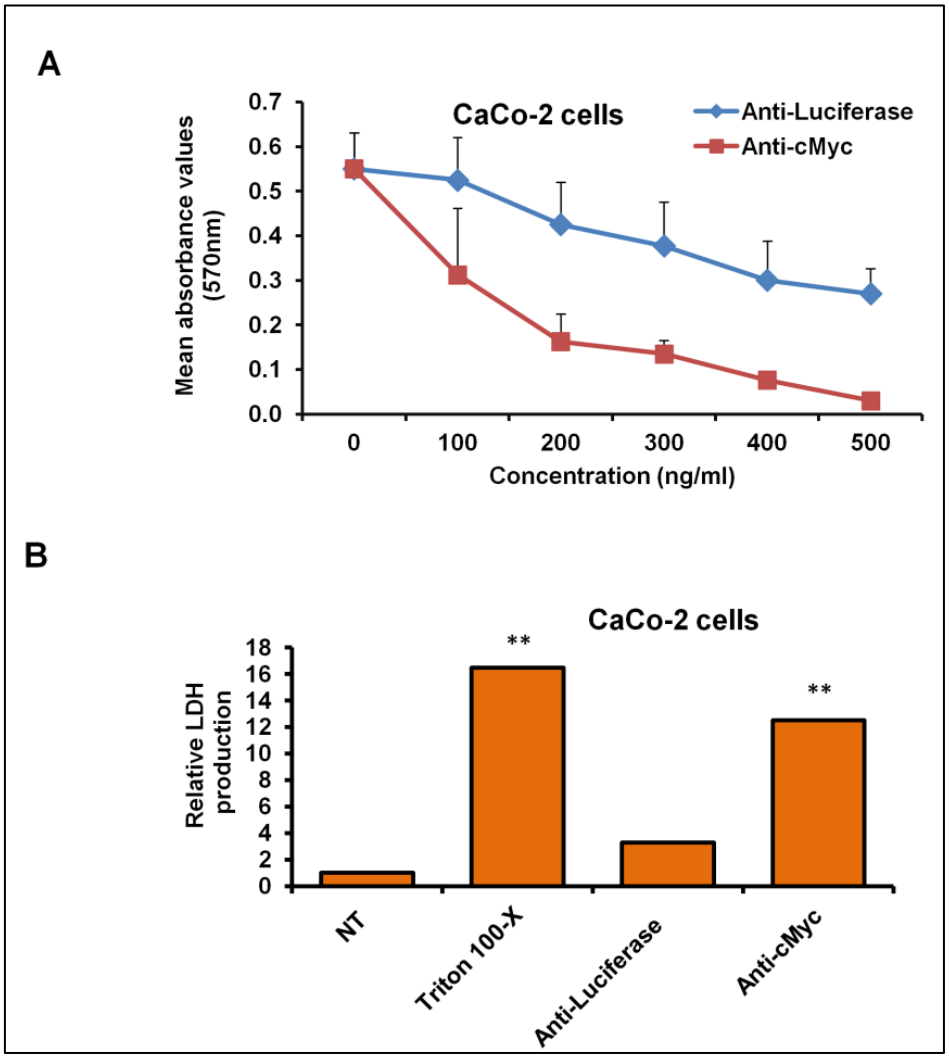

Figure 2: Cell viability and cytotoxic potential of siRNA transfection, (A) **Cell viability rate of CaCo-2 cells transfected with different doses of siRNA antagonist c-myc compared with cells transfected with the same doses of siRNA against Luciferase at 48 hrs post-transfection using MTT assay.** (B) **Relative LDH production from siRNA-transfected cells compared to Triton 100-X treated and nontreated cells (NT). Error bars indicate the standard deviation (SD) of four different replicates**. **The student's two tails *t*-test was used to determine the significance of differentiated values. (**) indicates the *P* ≤0.01**

Table 2: Cell viability rate of transfected CaCo-2 cells with siRNA targeting Luciferase and cMyc

Conditions	**Anti-Luciferase Concentration (ng/ml)**						**Anti-cMyc Concentration (ng/ml)**					
	0	**100**	**200**	**300**	**400**	**500**	**0**	**100**	**200**	**300**	**400**	**500**
Mean	0.55	0.53	0.43	0.38	0.30	0.27*	0.55	0.31**	0.16**	0.14**	0.08**	0.03**
STD	0.08	0.10	0.10	0.10	0.09	0.06	0.08	0.15	0.06	0.03	0.02	0.01
***P* values**		0.70	0.09	0.06	0.07	0.05		0.03	0.01	0.01	0.01	0.01

STD: Standard deviation

Table 3: Relative LDH production from CaCo-2 cells transfected with 100ng/ml of each siRNA

Conditions	NT	Triton 100-X	Anti-Luciferase	Anti-cMyc
Mean	0.01	0.17**	0.03	0.13*
STD	0.01	0.07	0.03	0.05
Relative LDH production	1.00	16.50	3.28	12.50
***P* values**		0.01	0.3063	0.0238

NT: Nontreated cells
STD: Standard deviation

Alteration of CaCo-2 cell morphology in cMyc knockdown cells

Cell morphology and the number of survived cells in transfected CaCo-2 cells were assessed and compared with transfected normal colon epithelial cells (NCM-460 cell line). Accordingly, both cell lines were cultured in a 6/well plate with 10x104 cells/well density. On day 2, the cells were transfected with 100ng/ml siRNA that antagonist either c-myc or Luciferase and incubated for two days. Markedly, the cell morphology obtained by the inverted microscope revealed distressing CaCo-2 cells transfected with siRNA antagonist c-myc, while showing a negligible effect on the transfected NCM-460 cell line (Figure 3A). Notable, the transfection of siRNA targeting Luciferase showed insignificant changes in the cell morphology of both transfected cells (Figure 3A). The number of surviving cells significantly decreased in response to transfection with siRNA antagonist c-myc only in CaCo-2 cells (Figure 3B and Table 4).. At the same time, the same concentration of siRNA antagonist Luciferase showed insufficient changes in the number of survived cells (Figure 3B and Table 4). These findings reveal the harmless effect of siRNA transfection in normal colon epithelial cells and provide evidence for the ability of siRNA antagonist c-myc to regulate cancer cell proliferation.

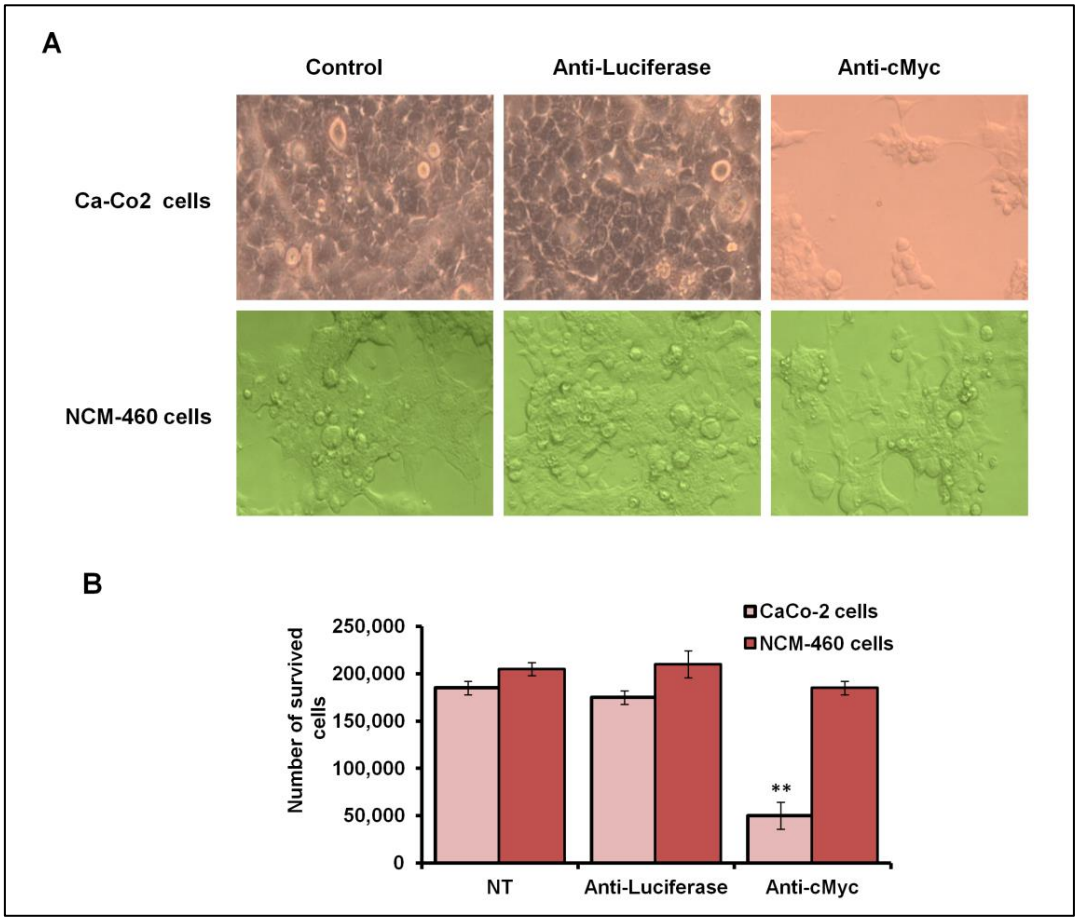

Figure 3: Cell morphology and number of survived cells in response to siRNA transfection, (A) Representative cell morphology obtained by the inverted microscopy illustrates cell viability of both CaCo-2 cells and NCM-460 cells that were transfected with 100 ng/ml of siRNA antagonist either c-myc or Luciferase for 24 hrs. (B) The number of living cells upon transfection with indicated siRNAs. Error bars indicate the standard deviation (SD) of three independent experiments. The student's two tails *t*-test was used to achieve the significance of calculated values. (*) indicates *P-values* ≤0.05, and (**) indicates the *P* ≤0.01

Table 4: Number of survived cells transfected with 100ng/ml of siRNA antagonist either Luciferase or c-myc gene

Conditions	CaCo-2 cells			NCM-460 cells		
	NT	**Anti-luciferase**	**Anti-c-myc**	**NT**	**Anti-luciferase**	**Anti-c-myc**
Mean	185000	175000	50000**	205000	210000	185000
STD	7071.068	7071.07	14142.14	7071.07	14142.14	7071.07
***P* values**		0.293	0.007		0.698	0.106

NT: Nontreated cells
STD: Standard deviation

Targeting c-myc coding sequence induces programmed cell death (PCD) via blocking Raf-1 gene expression

The knockdown efficiency of c-myc has been achieved in transfected cells using qRT-PCR. As shown in Figure 4A and Table 5, the relative gene expression of c-myc significantly reduced by more than 80% in cells transfected with anti-c-myc siRNA compared with its expression in control-transfected cells and nontreated cells. The *p*-value obtained by the statistical analysis of quantified c-myc-mRNA was equal to 0.01 in cells transfected with siRNA antagonist c-myc, indicating a highly significant difference in c-myc gene expression. Likewise, the relative gene expression of Raf-1 significantly downregulated in cells transfected with siRNA targeting c-myc, since *P* values were equal to 0.01 (Figure 4B and Table 5). These findings confirm the sufficient inhibition of c-myc gene expression by the transfection with the newly designed siRNA and suggest the correlation between c-myc expression and Raf-1 gene expression. To investigate the integration of c-myc knockdown in PCD of transfected CaCo-2 cells, the expression profile of the tumor suppressor gene, P53, and apoptotic transcription factor, Casp3, was assessed in transfected Caco-2 cells. Interestingly, the relative gene expression of both P53 and Casp3 dramatically upregulated to more than 7-fold change in CaCo-2 cells transfected with siRNA antagonist c-myc, compared with untreated and control-transfected cells (Figure 4C, D and Table 5). The statistical analysis in Table 5 clarified that the increase of P53 and Casp3 gene expression was highly significant since *P* values were equal to 0.01 and 0.001, respectively. Together, these data suggest that targeting c-myc with specific siRNA blocks the expression profile of Raf-1 and can induce PCD by increasing P53 and Casp3 gene expression.

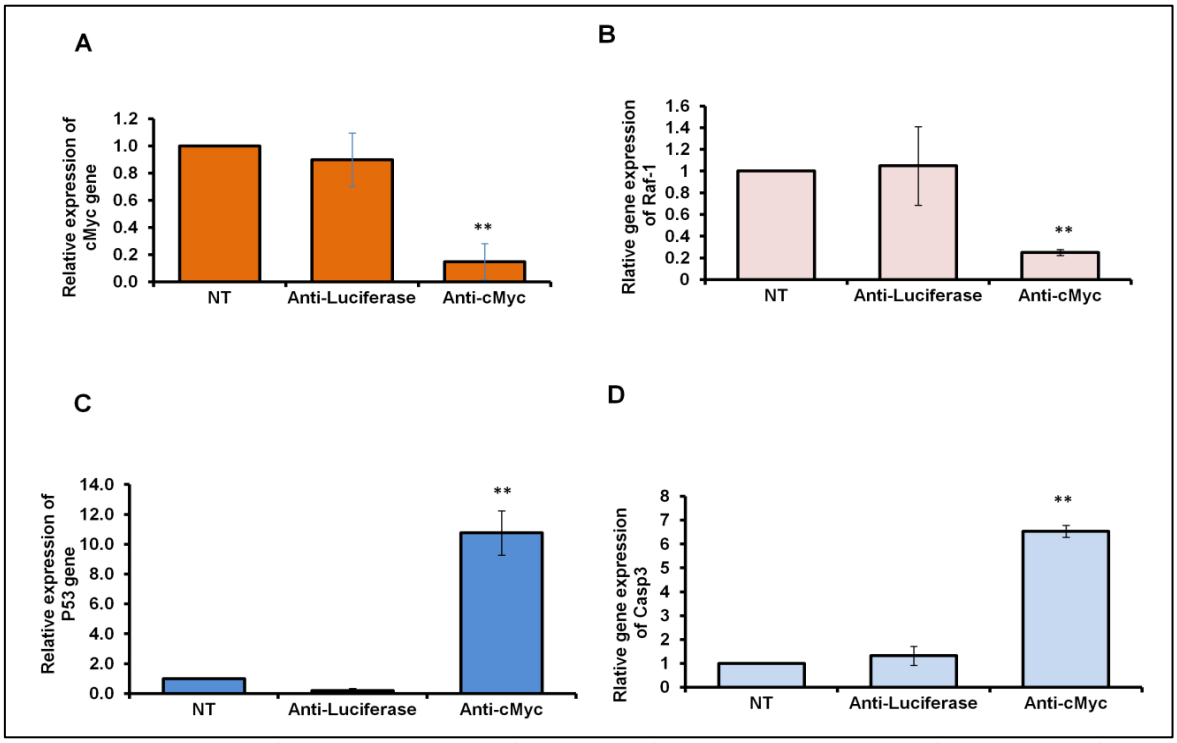

Figure 4: Relative gene expression of c-myc and its associated factors in transfected CaCo-2 cells, (A) **Quantification analysis of c-myc mRNA revealed the knockdown efficiency of c-myc indicated by fold change in transfected CaCo-2 cells compared with control-transfected cells and untreated cells (NT).** (B) **The mRNA expression level of the Raf-1 gene was quantified as indicated by fold change in transfected Caco-2 cells compared with untreated cells (NT) and control-transected cells.** (C and D) **Relative gene expression of cell death-related factors, P53 and Casp3, in transfected cells with respective siRNAs antagonists, either cMyc or Luciferase, compared with control-transfected cells. Error bars indicate the S.D. of two independent experiments. The student's two tails *t*-test was used to determine the significance of differentiated Ct values. (**) indicates the *P* ≤0.01**

Table 5: Quantification analysis of cMyc, Raf-1, P53, and Casp3 in siRNA-transfected cells

Genes	Condition	Expression fold changes	STD	Student two-tails t-test	*P*-values
cMyc	NT	1.00	0.00		
	Anti-Luciferase	0.9	0.19	0.53	< 0.05
	Anti-cMyc	0.15**	0.13	0.012	> 0.05
Raf-1	NT	1.00	0.00		
	Anti-Luciferase	1.04	0.15	0.36	< 0.05
	Anti-cMyc	0.24*	0.58	0.02	> 0.05
P53	NT	1	0.00		
	Anti-Luciferase	0.20**	0.14	0.01	≥ 0.01
	Anti-cMyc	10.7**	1.48	0.01	≥ 0.01
Casp-3	NT	1	0.00		
	Anti-Luciferase	1.32	0.4	0.73	< 0.05
	Anti-cMyc	6.53**	0.24	0.001	≥ 0.01

STD: Standard deviation

Antagonism cMyc gene expression regulates pro and anti-inflammatory cytokines

To state the correlation between c-myc knockdown and cytokines secretion, the level of produced IL-1α and IL-1β, as pro-inflammatory cytokines, were assessed in a time-course experiment following transfection with siRNA (100ng/ml). Moreover, the levels of produced IL-4 and IL-10, as anti-inflammatory cytokines, were monitored in transfected cells using an ELISA assay. Interestingly, the transfection of CaCo-2 cells with siRNA antagonist c-myc showed a high secretion level of both IL-1α and IL-1β in a time-dependent manner. Meanwhile, the concentration of produced IL-1α and IL-1β was constant during indicated time points following transfection in control-transfected and nontreated cells (Figure 5A and B). In contrast, the concentration of produced IL-4 and IL-10 markedly decreased in cells transfected with siRNA targeting c-myc in a time-dependent manner. However, IL-4 and IL-10 increased gradually at the early time points following transfection in control-transfected and nontreated cells (Figure 5C and D). These findings indicate the negative correlation between c-myc gene expression and pro and anti-inflammatory cytokines production and suggest the direct correlation between cMyc protein expression and cellular immune response.

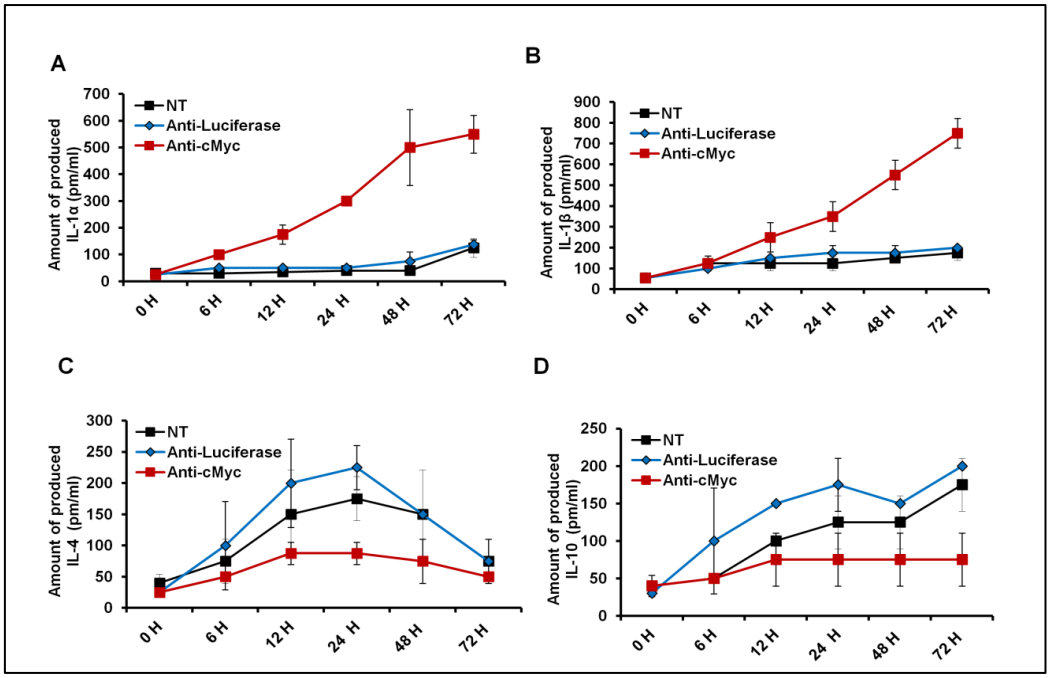

Figure 5: Levels of produced inflammatory cytokines in siRNA transfected cells, (A and B) **The concentration of produced IL-1α and IL1-β (pm/ml) in the fluids media of CaCo-2 cells transfected with 100ng/ml of each siRNA at the indicated time points compared with NT cells**. (C and D) **Level of produced IL-4 and IL10 (pm/ml) from Caco-2 cells transfected with 100ng/ml of each siRNA for the indicated time points compared with NT cells. Error bars reveal the SD of three replicates**

DISCUSSION

The regulation of cellular growth and metabolism are directly interrelated with c-myc gene expression. The c-myc oncogene is the crucial mediator controlling many factors involved in these processes (Morrish *et al*., 2008). The overexpression of cMyc protein is necessary during the metabolic changes in transformed cells to support the increasing requirement for nucleic acids, proteins, and lipids required for cell proliferation (Miller *et al*., 2012). In addition, cMyc protein overexpression is essential for coordinating changes in the expression level of many gene families that facilitate and support cellular proliferation. The cMyc protein influences malignancy transformation either as a primary oncogene, activated by amplification or translocation, or as a downstream target of other activated oncogenes. In both cases, it appears that cMyc plays a crucial role in maintaining the transformation changes. This exciting duality of cMyc protein makes it at the center of transformational changes and plays a vital role in controlling the "transformed phenotype." Although the effort of exploiting cMyc as a therapeutic target has been quite irritating, this may change in the next few years (Pelengaris *et al.*, 2002). The role of regulation cMyc protein in the cancer microenvironment of reduced energy supplies has been reported. The cancer cells are markedly disturbed in areas far from the blood vessels *in-vivo* and under oxygen- and glucose-depleted conditions *in-vitro*. The rapid decrease of c-Myc protein expression needs low levels of oxygen and glucose. Notably, repression of c-Myc protein levels by specific siRNA decreased the programmed cell death of necrotic cells induced by oxygen and glucose depletion. Thus, the environmental milieu resulted in regulation of c-Myc protein levels is a strategy for cancer cells to survive under conditions of limited energy sources (Okuyama *et al*., 2010). Based on that, this study was conducted to regulate c-myc gene expression with a respective siRNA antagonist its coding sequence in colon cancer cells, CaCo-2 cell lines. Notably, the transfection of the normal epithelial colon cells NCM-460 with the designed anti-c-myc siRNA did not reveal any cytotoxic effect. In contrast, the transfection of CaCo-2 cells showed significant alteration in cell morphology, cell viability, and the number of survived cells. This finding demonstrates the selective regulation of colon cancer cells by transfection with this siRNA that sufficiently inhibits c-myc gene expression.

Furthermore, The expression of the c-myc oncogene and its protein profile, c-Myc protein is mainly increased in almost malignant tumors (Nesbit *et al*., 1999). c-myc gene expression also occurs commonly in various cancers; in addition, the mutations in its coding region are rare in most types of malignancies, although they frequently occur in some types of lymphoma (Boxer and Dang, 2001). In general, the oncogenicity of c-myc needs an overexpression of this gene; however, the expression levels of c-myc in human cancers range from low to high, more than the normal range, as reported by Chung and Levens (Chung and Levens, 2005). These differences may not be unexpected since the c-Myc protein has versatile functions, including supporting cell proliferation and programmed cell death (PCD) (Meyer and Penn, 2008). It is possible that the c-Myc protein might be increased initially to support cancer initiation. However, it is later decreased to facilitate the tumor cell progression or to allow the tumor cell to adapt to changes in other genes for a survival purposes like what is occurred in the deficiency of the Apc gene (Felsher, 2010).

Noteworthy, the connection between c-myc expression and cellular inflammatory events has been reported in different types of cancer, including liver, lung, colon, and breast cancer (Xu *et al*., 2010; Madden *et al.*, 2021). For instance, in liver cancer, c-myc expression stimulates the expression of IL-8, IL-10, tumor necrosis factor-alpha (TNF-α), and transforming growth factor beta (TGF-β). Meanwhile, the upregulation of IL-1, IL-2, IL-4, TNF-α, and TGF-β promotes c-myc expression. These mediators play a central role in the dynamic force of many inflammatory liver disorders, which often result in fibrosis, cirrhosis, and liver tumorigenesis. Molecular interference of their interactions provides a therapeutic potential for chronic liver diseases (Liu *et al*., 2015). In this way, we further confirmed the link between c-myc gene expression and its knockdown efficiency with the production of IL-1α, IL1-β, IL-4, and IL10 in colon cancer cells. Mechanistically, the increasing levels of produced IL-1α and IL1-β may contribute to restoring the depleted c-myc in transfected CaCo-2 cells. Furthermore, the disturbance of c-myc gene expression reduced the level of produced IL-4 and IL10 due to their anti-inflammatory response in transfected CaCo-2 cells. These data confirm the crucial role of c-myc gene expression in regulating colon cancer cell proliferation and controlling the inflammatory event in colon cancer.

CONCLUSION

To check the possible impact of c-myc knockdown in colon cancer cell proliferation, we designed a respective siRNA antagonist c-myc coding sequence. Colon cancer cell line, CaCo-2 cells were transfected with the newly designed siRNA and compared with the transfected normal colon epithelial cells NCM-460. Targeting c-myc in CaCo-2 cells showed significant alteration in cell morphology and the number of survived cells following transfection. Compared with normal cells, targeting c-myc with the specific siRNA selectively regulated cancer cell proliferation and cell viability rate. Downregulation of c-myc in cancer cells has been implicated in decreasing Raf-1 gene expression while increasing the expression of P53 and Caspase 3 as indicators for programmed cell death. Likewise, targeting c-myc in colon cancer cells resulted in the overproduction of the proinflammatory,

including IL-1α and IL-β, while decreasing the production of anti-inflammatory cytokines, including IL-4 and IL-10. These data provide evidence for the biological role of c-myc gene expression in colon cancer proliferation and the inflammatory event accompanying tumourigenesis.

Authors' Contributions

Yousry Atef provided the experiments. Nasser Abbas and Adel Guirgis helped in supervision, data analysis and writing the manuscript. Hany Khalil designed the research plan, supervised overall research, provided and interpreted data and wrote the manuscript.

Availability of data and materials

The data supporting this study's findings are available from the corresponding author upon reasonable request.

Conflicts of interest: All authors declare that there are no conflicts of interest.

REFERENCES

- Abd El Maksoud, A. I., Elebeedy, D., Abass, N. H., Awad, A. M., Nasr, G. M., Roshdy, T., et al. (2020). Methylomic Changes of Autophagy-Related Genes by Legionella Effector Lpg2936 in Infected Macrophages. *Front. Cell Dev. Biol.* 7, 390. doi:10.3389/fcell.2019.00390.
- Abd El Maksoud, A. I., Taher, R. F., Gaara, A. H., Abdelrazik, E., Keshk, O. S., Elawdan, K. A., et al. (2019). Selective Regulation of B-Raf Dependent K-Ras/Mitogen-Activated Protein by Natural Occurring Multi-kinase Inhibitors in Cancer Cells. *Front. Oncol.* 9, 1220. doi:10.3389/fonc.2019.01220.
- Bellovin, D. I., Das, B., and Felsher, D. W. (2013). "Tumor Dormancy, Oncogene Addiction, Cellular Senescence, and Self-Renewal Programs BT - Systems Biology of Tumor Dormancy," in, eds. H. Enderling, N. Almog, and L. Hlatky (New York, NY: Springer New York), 91–107. doi:10.1007/978-1-4614-1445-2_6.
- Black, A. R., and Black, J. D. (2013). Protein kinase C signaling and cell cycle regulation. *Front. Immunol.* 3, 423. doi:10.3389/fimmu.2012.00423.
- Boxer, L. M., and Dang, C. V (2001). Translocations involving c-myc and c-myc function. *Oncogene* 20, 5595–5610. doi:10.1038/sj.onc.1204595.
- Chung, H.-J., and Levens, D. (2005). c-myc Expression: Keep the Noise Down! *Mol. Cells* 20, 157–166. Available at: https://molcells.org/journal/view.html?doi=.
- Devenport, S. N., and Shah, Y. M. (2019). Functions and Implications of Autophagy in Colon Cancer. *Cells* 8, 1349. doi:10.3390/cells8111349.
- El-Fadl, H. M. A., Hagag, N. M., El-Shafei, R. A., Khayri, M. H., El-Gedawy, G., Maksoud, A. I. A. El, et al. (2021). Effective Targeting of Raf-1 and Its Associated Autophagy by Novel Extracted Peptide for Treating Breast Cancer Cells. *Front. Oncol.* 11, 3317. doi:10.3389/fonc.2021.682596.
- Elimam, H., El-Say, K. M., Cybulsky, A. V, and Khalil, H. (2020). Regulation of Autophagy Progress via Lysosomal Depletion by Fluvastatin Nanoparticle Treatment in Breast Cancer Cells. *ACS Omega*. doi:10.1021/acsomega.0c01618.
- Felsher, D. W. (2010). MYC Inactivation Elicits Oncogene Addiction through Both Tumor Cell–Intrinsic and Host-Dependent Mechanisms. *Genes Cancer* 1, 597–604. doi:10.1177/1947601910377798.
- Hamouda, R. A., Abd El Maksoud, A. I., Wageed, M., Alotaibi, A. S., Elebeedy, D., Khalil, H., et al. (2021). Characterization and Anticancer Activity of Biosynthesized Au/Cellulose Nanocomposite from Chlorella vulgaris. *Polymers (Basel).* 13. doi:10.3390/polym13193340.
- Islam, S. M. A., Patel, R., and Acevedo-Duncan, M. (2018). Protein Kinase C-ζ stimulates colorectal cancer cell carcinogenesis via PKC-ζ/Rac1/Pak1/β-Catenin signaling cascade. *Biochim. Biophys. Acta - Mol. Cell Res.* 1865, 650–664. doi:https://doi.org/10.1016/j.bbamcr.2018.02.002.
- Khalil, H. (2012). Influenza A virus stimulates autophagy to undermine host cell IFN-β production. *Egypt. J. Biochem. Mol. Biol.* 30, 283–299.
- Khalil, H., Abd El Maksoud, A. I., Roshdey, T., and El-Masry, S. (2019). Guava flavonoid glycosides prevent influenza A virus infection via rescue of P53 activity. *J. Med. Virol.* 91, 45–55. doi:10.1002/jmv.25295.
- Khalil, H., Arfa, M., El-Masrey, S., EL-Sherbini, S., and Abd-Elaziz, A. (2017a). Single nucleotide polymorphisms of interleukins associated with hepatitis C virus infection in Egypt. *J. Infect. Dev. Ctries.* 11, 261–268. doi:10.3855/jidc.8127.
- Khalil, H., El Malah, T., El Maksoud, A. I. A., El Halfawy, I., El Rashedy, A. A., and El Hefnawy, M. (2017b). Identification of novel and efficacious chemical compounds that disturb influenza A virus entry in vitro. *Front. Cell. Infect. Microbiol.* doi:10.3389/fcimb.2017.00304.
- Khalil H, Arfa M, El-Masrey S, EL-Sherbini S, and Abd-Elaziz A. (2017). Single nucleotide polymorphisms of interleukins associated with hepatitis C virus infection in Egypt. *J. Infect. Dev. Ctries.* 11, 261–268. doi:10.3855/jidc.8127.
- Levens, D. (2010). "You Don't Muck with MYC." *Genes Cancer* 1, 547–554. doi:10.1177/1947601910377492.
- Liu, T., Zhou, Y., Ko, K. S., and Yang, H. (2015). Interactions between Myc and Mediators of Inflammation in Chronic Liver Diseases. *Mediators Inflamm.* 2015, 276850. doi:10.1155/2015/276850.
- Madden, S. K., de Araujo, A. D., Gerhardt, M.,

Fairlie, D. P., and Mason, J. M. (2021). Taking the Myc out of cancer: toward therapeutic strategies to directly inhibit c-Myc. *Mol. Cancer* 20, 3. doi:10.1186/s12943-020-01291-6.

- Maher, E., Gedawy, G., Fathy, W., Farouk, S., El Maksoud, A. A., Guirgis, A. A., et al. (2020). Hsa-miR-21-mediated cell death and tumor metastases: A potential dual response during colorectal cancer development. *Middle East J. Cancer* 11. doi:10.30476/mejc.2020.83146.1139.
- Meyer, N., and Penn, L. Z. (2008). Reflecting on 25 years with MYC. *Nat. Rev. Cancer* 8, 976–990. doi:10.1038/nrc2231.
- Miller, D. M., Thomas, S. D., Islam, A., Muench, D., and Sedoris, K. (2012). c-Myc and Cancer Metabolism. *Clin. Cancer Res.* 18, 5546–5553. doi:10.1158/1078-0432.CCR-12-0977.
- Mohamed, E.-S. A., Bassiouny, K., Alshambky, A. A., and Khalil, H. (2022). Anticancer Properties of N,N-dibenzylasparagine as an Asparagine (Asp) analog, Using Colon Cancer Caco-2 Cell Line. *Asian Pacific J. Cancer Prev.* 23, 2531–2540. doi:10.31557/APJCP.2022.23.7.2531.
- Morrish, F., Neretti, N., Sedivy, J. M., and Hockenbery, D. M. (2008). The oncogene c-Myc coordinates regulation of metabolic networks to enable rapid cell cycle entry. *Cell Cycle* 7, 1054–1066. doi:10.4161/cc.7.8.5739.
- Nesbit, C. E., Tersak, J. M., and Prochownik, E. V (1999). MYC oncogenes and human neoplastic disease. *Oncogene* 18, 3004–3016. doi:10.1038/sj.onc.1202746.
- Okuyama, H., Endo, H., Akashika, T., Kato, K., & Inoue, M. (2010). Downregulation of c-MYC Protein Levels Contributes to Cancer Cell Survival under Dual Deficiency of Oxygen and Glucose. *Cancer Res.* 70, 10213–10223. doi:10.1158/0008-5472.CAN-10-2720.
- Pelengaris, S., Khan, M., and Evan, G. (2002). c-MYC: more than just a matter of life and death. *Nat. Rev. Cancer* 2, 764–776. doi:10.1038/nrc904.
- Rao, X., Huang, X., Zhou, Z., and Lin, X. (2013). An improvement of the2–delta delta CT) method for quantitative real-time polymerase chain reaction data analysis. *Biostat Bioinforma Biomath.* doi:10.1016/j.micinf.2011.07.011.Innate.
- Taher, R. F., Al-Karmalawy, A. A., Abd El Maksoud, A. I., Khalil, H., Hassan, A., El-Khrisy, E.-D. A., et al. (2021). Two new flavonoids and anticancer activity of Hymenosporum flavum: in vitro and molecular docking studies. *J Herbmed Pharmacol* 10, 443–458. doi:10.34172/jhp.2021.52.
- Xu, J., Chen, Y., and Olopade, O. I. (2010). MYC and Breast Cancer. *Genes Cancer* 1, 629–640. doi:10.1177/1947601910378691.
- Zhao, Q., Assimopoulou, A. N., Klauck, S. M., Damianakos, H., Chinou, I., Kretschmer, N., et al. (2015). Inhibition of c-MYC with involvement of ERK/JNK/MAPK and AKT pathways as a novel mechanism for shikonin and its derivatives in killing leukemia cells. *Oncotarget; Vol 6, No 36*. Available at: https://www.oncotarget.com/article/5380/text/.